IIETA International Information and Engineering Technology Association
Advancing the World of Information and Engineering

Mathematical Modelling of Engineering Problems
Vol. 10, No. 6, December, 2023, pp. 1961-1966
Journal homepage: http://iieta.org/journals/mmep

Experimental and Numerical Investigation on the Free Vibration Characteristics of 3D Printed Springs with Square Cross Sections

Hassan Hamoodi Mahdi[1*], Sami Ali Nama[1], Sulaiman Mustafa Khazaal[2]

[1] Engineering Technical College/Baghdad, Middle Technical University, Baghdad 10074, Iraq
[2] Faculty of Mechanical Engineering and Informatics, University of Miskolc, Miskolc 3530, Hungary

Corresponding Author Email: dr_hassan1961@yahoo.com

https://doi.org/10.18280/mmep.100605

Received: 11 April 2023
Revised: 15 June 2023
Accepted: 11 July 2023
Available online: 21 December 2023

Keywords:
3D printed, rectangular spring, machined spring, free vibration, SolidWorks

ABSTRACT

In the present study, a spring with a square cross-section was fabricated utilizing 3D printing technology. An extensive examination of the free vibration characteristics of these printed springs was carried out, both experimentally and numerically. Three distinct infill patterns (Octet, Triangle, and Cross), three varying infill percentages (50%, 60%, and 80%), and three different numbers of coils (one, two, and four coils) were scrutinized. Furthermore, an additional three samples, each exhibiting 100% infill with the Octet pattern, were printed to represent the solid model of the spring, each having one, two, and four coils respectively. The stiffness, shear modulus, and material density of the fabricated springs were computed experimentally. Subsequently, springs with different configurations were modeled and subjected to analysis using SolidWorks 2018. The results reveal that for the case with 100% infill, the spring stiffness amplifies fourfold and sixteen fold respectively for two and four coils, when compared with the one-coil printed spring. Simultaneously, the fundamental frequency exhibited a twofold and fourfold increase respectively. Springs fabricated with an 80% Octet pattern exhibited a higher fundamental frequency than those printed with Triangle or Cross patterns. This study, therefore, provides valuable insights into the influence of infill patterns, infill percentages, and coil numbers on the vibration characteristics of 3D printed springs.

1. INTRODUCTION

Springs, due to their inherent capacity for energy storage and resilience, are vital components in mechanical engineering. Their unique property, which allows them to revert to their original form following the removal of an applied force, has resulted in a broad spectrum of applications encompassing toys, measurement devices, timepieces, bicycles, shock absorbers, and vibration controllers. Historically manufactured from spring steel, recent advancements have led to the inclusion of a myriad of other materials, such as graphite epoxy used in leaf springs, carbon epoxy crafted from carbon fibers for automotive applications, and chromium alloy, recognized for its superior heat resistance and strength, and implemented in the fabrication of springs with rectangular cross-sections.

Over the years, springs have been the subject of rigorous investigation. Both analytical and experimental methods have been applied to study the impact of various materials on their mechanical and vibrational characteristics [1-5].

Despite offering enhanced flexibility within confined spaces, rectangular springs often transform from a square cross-section shape into a trapezoid during the spiral formation process. This change in form has been observed to diminish the shock absorption capacity of the springs [6, 7]. In contrast to traditional springs that predominantly contain a single coil configuration and necessitate special attachments, machined springs can be designed to encompass multiple coils [8]. Precisely engineered from a single piece, machined springs maintain their specifications and can manifest as compression, tension, or torsional springs [9-15].

The advent of 3D printing technology has revolutionized the production of complex shapes previously unattainable through conventional methods. A multitude of materials, including diverse types of plastic, metals, and even biological cells, can be manipulated through this technology [16-18]. The quality of the printed objects is determined by a range of parameters such as the infill pattern and percentage, printing speed and temperature, type of material employed, and the diameter of the printing nozzle. The infill percentage has been found to influence aspects such as the elastic modulus, tensile and compressive strength, and printing time [19, 20]. Numerous infill patterns exist, including line, triangle, honeycomb, octet, and cross, with the choice of pattern and layer thickness impacting the printing time and the mechanical strength of the final product [21-24].

The importance of studying the free vibration analysis of 3D printed springs cannot be overstated. Such analysis is instrumental in optimizing performance, circumventing resonance issues, assessing durability, validating designs, and

enabling structural health monitoring. It provides a crucial understanding of the springs' dynamic behavior and characteristics, assisting engineers in making informed decisions during all stages of design, manufacturing, and operation.

This study sets out to examine the effect of printing parameters such as the infill pattern, infill percentage, and the number of coils on the fundamental frequency of 3D printed springs, both experimentally and numerically. The findings from this research are expected to extend the current understanding of the vibrational characteristics of 3D printed springs and contribute to the optimization of their design and performance.

2. THEORY

For a helical spring with rectangular wire, the fundamental frequency can be defined as [7]:

$$f_n = \frac{1}{2\pi}\sqrt{\frac{K}{M}} \quad (1)$$

$$K = \frac{F}{\delta} \quad (2)$$

$$K = \frac{G * a^4}{5.568 * N * D^3} \quad (3)$$

From Eqs. (2) and (3), the shear modulus can be defined as:

$$G = \frac{5.568 * F * N * D^3}{a^4 * \delta} \quad (4)$$

where:

f_n =Natural frequency (Hertz)
K=Spring stiffness (N/m)
M=Spring mass (Kg)
F=applied force (N)
δ=Deflection (mm)
G=Shear modulus of rigidity (N/mm^2)
a=length of spring side (mm)
N=number of spring coils.
D=spring mean diameter (mm)

3. EXPERIMENTAL WORK

Springs were printed with (Creality3D Ender-7) 3D Printer according to the printing parameters listed in Table 1. Twenty-seven spring specimens were printed in three different configurations (one coil, two coils, and four coils). For each configuration three infill pattern were used (Cross, Octet, Triangle) while for each pattern there was three infill percentage (50%, 60%, 80%) as shown in Figures 1-3 respectively.

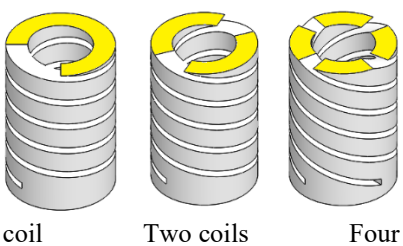

Figure 1. Printed spring with different configurations

To distinguish between the different infill pattern, three different filaments colors were used to print the springs as shown in Figure 4. Finally, extra three springs were printed with (one, two, and four coils), each of them with (Octet infill pattern and 100% infill percentage) to represent the solid model of the spring.

The (INSTRON) universal testing machine was used to conduct a compression test for the printed spring specimens and obtain the (Load/Extension) results for each value and from which the experimental spring stiffness was estimated. Using Eq. (4), the experimental shear modulus can be calculated. The mass of each printed spring is measured using a sensitive scale, from the mass value we can calculate the equivalent material density and from Eq. (1) we can obtain the fundamental natural frequency for each spring.

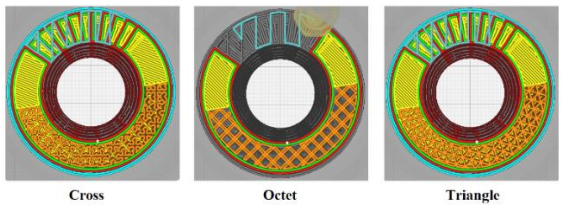

Figure 2. Different infill pattern

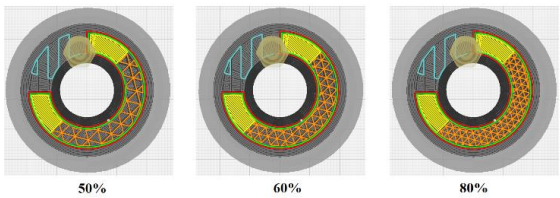

Figure 3. Different infill percentage for one-coil spring

Figure 4. Spring with one, two, and four coils (octet infill pattern and 100% infill percentage)

Table 1. Printing parameters

Property	Value
Filament type	PLA
Slicer software	Ultimaker Cura V 5.2.1
Layer height	0.15 mm
Wall thickness	1.5 mm
Top/bottom thickness	1 mm
Top layers	2
Bottom layers	2
Infill density	50%, 60%, 80%, 100%
Infill type	Triangle, Cross, Octet
Temperature	245℃
Build plate temperature	65℃
Print speed	50 mm/s
Support	OK

4. NUMERICAL MODELING

SolidWorks is a computer-aided design (CAD) software. It provides a comprehensive set of tools for designing, modeling, simulating, and documenting 3D mechanical and electrical systems. With SolidWorks, users can create 3D solid models of parts, assemble the individual parts into complex assemblies, and perform structural simulation analysis to evaluate the performance and behavior of designs.

SolidWorks 2018 was used to model and analyze the different configurations of the spring. The spring was modeled as a hollow cylinder with 30mm outer diameter, 18mm inner diameter, and 74mm height. A rectangular cut (2×6 mm) was made along a helical path containing 8 revolutions with 8mm pitch. The spring material was defined as custom material with Young's modulus=3530 MPa, Poisson's ratio=0.3, Tensile strength=50 MPa [25]. Shear modulus and mass density varies depending on printing infill percentage and infill pattern. As a boundary conditions, the spring was fixed from one end and free in the other end. The spring was meshed by solid high-quality mesh type with element size=2.5mm, total elements=17422, and total nodes=30533.

To verify a model, the experimental shear modulus and mass density values of the printed spring were defined for the spring material. Static study was conducted with a force applied to the free edge of the spring model and the resulting displacement and fundamental frequency were compared with the experimental results.

To study the effect of printing infill percentage and infill pattern on the fundamental frequency, The shear modulus and mass density values were assigned according to the experimental results for the infill pattern and infill percentage for each case.

Finally, to study the effect of number of spring coils on the fundamental natural frequency, two rectangular shapes (each of 2x6 mm) were cut from the hollow cylinder along two helical paths each of them contains 4 revolutions with 16mm pitch to model a spring with two coils (distributed in two opposite locations along the spring mean diameter), while the four coils spring was modeled by cutting four rectangular shapes along four helical paths each of them contains 2 revolutions with 32mm pitch.

5. RESULTS AND DISCUSSION

The experimental and numerical work was done for several printed springs. The effect of the infill percentage, infill pattern, and number of coils on the fundamental frequency were studied. The experimental results for the variation of the fundamental frequency at different infill percentage for the Octet, Triangles, and Cross infill patterns for springs with one, two, and four coils are shown in Figures 5-7, while Figures 8-10 shows the comparison between the experimental and numerical fundamental frequency results at different infill percentage for the different infill patterns and different number of coils.

To calculate the stiffness of a 3D printed spring experimentally, it was attached to the tensile testing machine and apply known loads incrementally. The corresponding deformations or displacements of the spring for each load increment was measured to get its load-deformation curve. The stiffness (k) of the spring was determined from the slope of the linear region of the load-deformation curve. The shear modulus (G) was determined experimentally from the slope of the linear region of the stress-strain curve of the printed spring.

The experimental mass, stiffness, and fundamental frequency results for the spring with one coil and Octet infill pattern are listed in Table 2. It can be noted that the fundamental frequency is higher for 80% infill percentage than that of 100% although there is a decrease in mass value, while it is decreases as the mass decreases for 60 and 50%infill. The reason for that is the effect of increasing in stiffness on the fundamental frequency is more than the effect of decreasing the mass value for the 80% spring, while for the 60% and 50% both mass and stiffness decreases in a manner that decreases the fundamental frequency. The increase in fundamental frequency is about (1.5 Hz) and represents about 3.5% improvement in frequency from that of 100%. The other infill patterns have the same behavior as shown in Figure 5. The Octet and Triangle patterns are close in their weight content, and both of them are higher than Cross pattern.

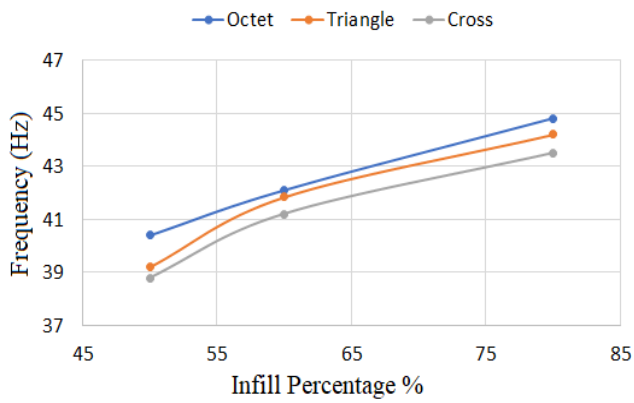

Figure 5. Effect of infill percentage on fundamental frequency at different infill pattern (One coil spring)

Table 2. Experimental results for octet one-coil spring at different infill percentages

Infill %	Mass (gram)	K (N/m)	f_n (Hz)
100	29.10	2.147	43.23
80	27.676	2.193	44.8
60	25.612	1.792	42.1
50	23.807	1.534	40.4

For the spring with two coils and Octet infill pattern, the experimental mass, stiffness, and fundamental frequency results are listed in Table 3. It can be noted again that the fundamental frequency for 80% infill is higher than that of 100% while it is lower for 60% and 50% infill, this can be again related to the increase in spring stiffness. To compare these results with that of one-coil spring, the results in Table 3 showed that the stiffness values are 7.745 and 9.096 N/m for 100% and 80% respectively. The increase in stiffness is about (3.61 and 4.15 times) greater than that of one-coil spring which in turn results in increasing the fundamental frequency up to (82.21 and 89.6 Hz), this represents an improvement of (190% and 207%) in the fundamental frequency. Figure 6 shows the behavior of the other two infill patterns at different infill percentages, again it can be noted that the Octet infill pattern gives higher results compared with the Triangle and Cross patterns.

Table 3. Experimental results for octet two-coils spring at different infill percentages

Infill %	Mass (gram)	K (N/m)	f_n (Hz)
100	29.024	7.745	82.21
80	28.699	9.096	89.6
60	27.519	6.849	79.4
50	26.471	5.091	69.8

For the spring with four coils and Octet infill pattern, the experimental results are listed in Table 4. The same behavior can be noted for the different infill percentages as that for the one coil and two coils springs. The stiffness values are (38.471 and 40.585 N/m) for 100% and 80% infill respectively and the increase in stiffness is about (17.9 and 18.5 times) greater than that of one-coil spring. The fundamental frequency increases up to (180.88 and 190.87 Hz), this results in an improvement of (418% and 426%) in the fundamental frequency. The behavior of the Triangle and Cross infill patterns at different infill percentages is shown in Figure 7, again it can be noted that the Octet infill pattern gives the highest results while the Cross pattern shows the lowest results.

Table 4. Experimental results for octet four-coils spring at different infill percentages

Infill %	Mass (Gram)	K (N/m)	f_n (Hz)
100	29.785	38.471	180.88
80	28.218	40.585	190.87
60	27.634	33.410	175
50	26.372	26.354	159.1

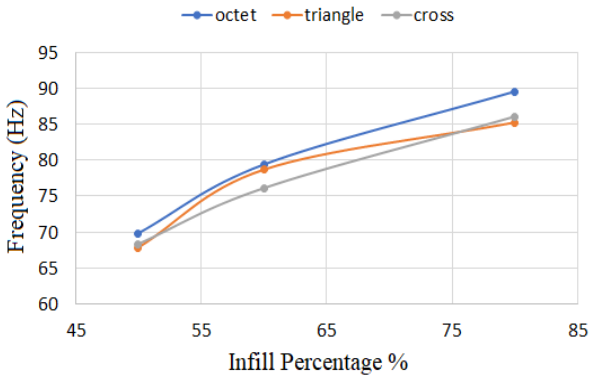

Figure 6. Effect of fundamental frequency with infill percentage at different infill pattern (Two coils spring)

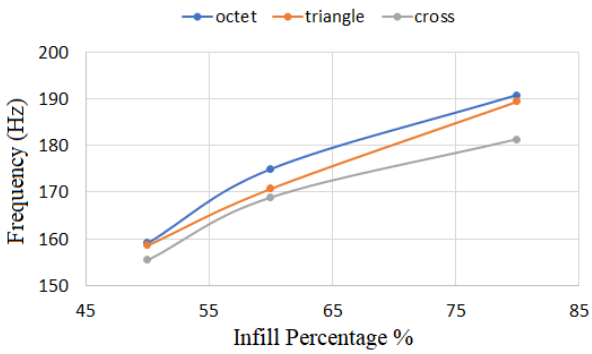

Figure 7. Effect of infill percentage on fundamental frequency at different infill pattern (Four coils spring)

Figures 8-10 show the comparison between the experimental and numerical fundamental frequency results of the printed springs with different infill percentage, different infill pattern and different number of coils. The behavior of the numerical results is similar to those of the experimental ones, the fundamental frequency decreases with the decrease in the infill percentage for the different filling patterns while the stiffness increases with the increase in the number of coils. The numerical values were less than the experimental values as a result of the assumption that the printed springs have a solid cross section and a variable density which depends on the weight of the spring, while the area cross section contains spaces as was shown in Figures 2 and 3. Table 5 lists the experimental and numerical results for the fundamental frequency of the different spring configurations.

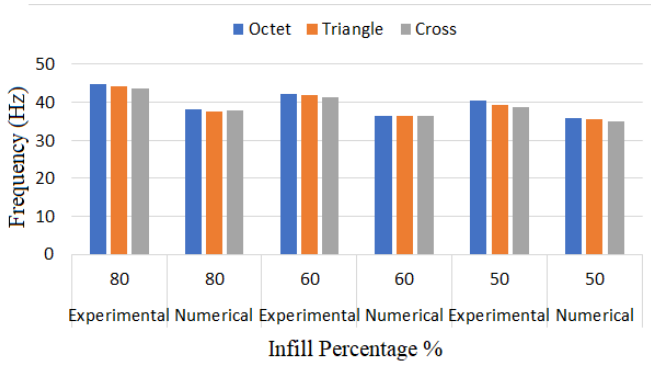

Figure 8. Numerical and experiment result of fundamental frequency (One coil spring)

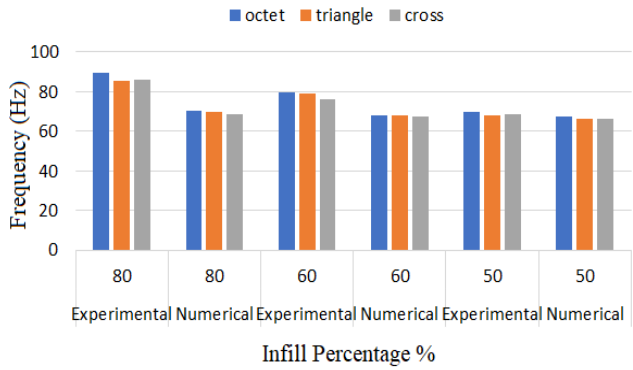

Figure 9. Numerical and experiment result of fundamental frequency (Two coils spring)

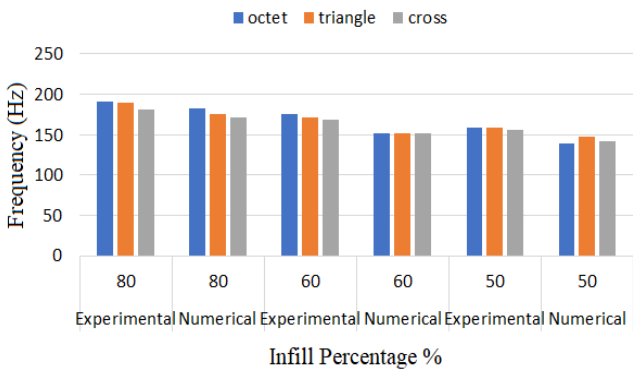

Figure 10. Numerical and experiment result of fundamental frequency (Four coils spring)

Table 5. Experimental and numerical fundamental frequency (Hz) results for different springs

No. of Coils	Infill Pattern	Infill Percentage								
		80%			60%			50%		
		Exp.	Num.	% Error	Exp.	Num.	% Error	Exp.	Num.	% Error
One Coil	Octet	44.8	37.94	18.08	42.1	36.44	13.44	40.4	35.89	11.16
	Triangle	44.2	37.63	17.46	41.84	36.39	13.03	39.2	35.51	9.41
	Cross	43.5	37.75	15.23	41.2	36.39	11.67	38.78	34.99	9.77
Two Coils	Octet	89.6	70.2	21.65	79.4	68.17	14.14	69.8	67.13	3.83
	Triangle	85.3	69.7	18.29	78.7	68.04	13.55	67.8	66.07	2.55
	Cross	86.1	68.61	20.31	76.1	67.29	11.58	68.3	65.89	3.53
Four Coils	Octet	190.87	181.7	4.80	175	151.4	13.49	159.1	139.1	12.57
	Triangle	189.5	174.7	7.81	170.8	150.8	11.71	158.65	147.8	6.84
	Cross	181.4	171.7	5.35	168.9	152	10.01	155.4	141.6	8.88

6. CONCLUSIONS

i. An analysis of the experimental and numerical findings revealed a maximum discrepancy of 21.65%, underscoring the need for further refinement in the experimental design or numerical modelling.

ii. When considering infill patterns, the Octet pattern was found to yield a higher fundamental frequency compared to the Triangle or Cross patterns. This suggests that the Octet pattern may offer superior mechanical properties for 3D printed springs.

iii. An 80% infill was observed to result in a higher fundamental frequency relative to other tested infill percentages. This indicates the potential benefits of using a higher infill percentage in enhancing the vibrational performance of the springs.

iv. In the case of springs printed with 100% infill, it was found that a spring with two coils exhibited a stiffness fourfold that of a spring with a single coil. Moreover, a spring with four coils demonstrated a stiffness approximately sixteen times that of a single-coil spring. This highlights the significant impact of coil number on the stiffness of 3D printed springs.

v. Similarly, for springs printed with 100% infill, the fundamental frequency of a two-coil spring was observed to be twice as high as that of a single-coil spring, while a four-coil spring exhibited a fundamental frequency approximately fourfold that of a single-coil spring. This underlines the importance of coil number in determining the vibrational characteristics of 3D printed springs.

vi. This study demonstrated the potential of 3D printing technology in manufacturing complex products such as multi-coil springs. The results suggest that with careful control of the printing parameters and design features, 3D printing can serve as a viable approach for creating customized springs with desirable mechanical properties.

REFERENCES

[1] Muhanad H.M., Nabeel A., Khaldoon H.H. (2020). Numerical investigation to optimizing the design of helical compression spring by using hollow shaft. Journal of Green Engineering (JGE), 10(7): 3832-3843.

[2] Choube, A.M., Sambhe, R.U. (2020). Stress analysis of square and rectangular cross section helical spring. International Journal of Scientific Research in Science, Engineering and Technology, 7(2): 362-367. https://doi.org/10.32628/IJSRSET207281

[3] Lubombo, C., Huneault, M.A. (2018). Effect of infill patterns on the mechanical performance of lightweight 3D printed cellular PLA parts. Journal of Materials Today Communications, 17: 214-228. https://doi.org/10.1016/j.mtcomm.2018.09.017

[4] Fernandez-Vicente, M., Caile, W., Ferrandiz, S., Conejero, A. (2016). Effect of infill parameters on tensile mechanical behavior in desktop 3D printing. 3D Printing and Additive Manufacturing, 3(3): 183-192. https://doi.org/10.1089/3dp.2015.0036

[5] Patel D. (2017). Effects of infill patterns on time, surface roughness and tensile strength in 3D printing. International Journal of Engineering Development and Research, 5(3): 566-569.

[6] Wahl, A.M. (1979). Mechanical Springs. 2nd edition, McGraw-Hill Inc., New York.

[7] Khurmi, R.S., Gupta, J.K. (2005). A Textbook of Machine Design. 14the edition, Eurasia Publishing House (PVT) LTD.

[8] Machined springs, retrieved from https://www.abssac.co.uk/c/Machined+Springs/17/, accessed on 20/2/2023.

[9] Nama, S.A. (2015). Modeling and analysis of a helical machined springs. The Iraqi Journal for Mechanical and Material Engineering, 15(2): 152-163.

[10] Nama, S.A. (2015). Effect of pitch angle on static characteristics of a helical machined spring. The Iraqi Journal for Mechanical and Material Engineering, 15(3): 181-190.

[11] Ahmed, I.R., Hani, A.A., Kadhim, M.M. (2013). Static and dynamic characteristics of slotted cylinder spring. International Journal of Engineering Research & Technology, 2(12): 3860-3871.

[12] Ahmed, I.R., Hani, A.A., Kadhim, M.M. (2014). Compression and impact characterization of helical and slotted cylinder springs. International Journal of Engineering & Technology, 3(2): 268-278. https://doi.org/10.14419/ijet.v3i2.2492

[13] de Dios Calderon, J., Perez, C. (2013). On the general characterization of machined springs and their manufacturing processes. ASME International Mechnical Engineering Congress and Exposition, Systems and Design, California, USA. https://doi.org/10.1115/IMECE2013-63402

[14] Krzysztof, M. (2006). Stress analysis in slotted springs. Mechanics, 25(3): 131-134.

[15] Salwinski, J., Michalczyk, K. (2006). Stress analysis in helical springs with closed end coils machined from cylindrical sleeves. Mechanics, 25(4): 169-172.

[16] Tho, N., Minh, T., Tai, N. (2020). The effect of infill pattern, infill density, printing speed and temperature on the additive manufacturing process based on the FDM technology for the hook-shaped components. Journal of Polimesin, 18(1): 1-6. http://doi.org/10.30811/jpl.v18i1.1445

[17] Lalegani, M., Ariffin, M. (2020). The effects of combined infill patterns on mechanical properties in FDM process. Polymers, 12(12): 1-20. https://doi.org/10.3390/polym12122792

[18] Nouman, F.E., Nama, S.A., Mahdi, H.H. (2021). Effect of infill percentage for 3D printed dies on spring back for aluminum sheets. International Journal on Technical and Physical Problems of Engineering (IJTPE), 13(4): 27-32.

[19] Baig, A., Moeed, K., Haque, M. (2019). A study on the effect of infill percentage and infill pattern on the compressive behavior of the FDM printed polylactic acid (PLA) polymer. Global Research and Development Journal for Engineering, 4(9): 5-8.

[20] Rismalia, M., Hidajat, S., Permana, G., Hadisujoto, B., Muslimin, M., Triawan, F. (2019). Infill pattern and density effects on the tensile properties of 3D printed PLA material. Journal of Physics, Conference Series, 1402(4): 1-6. https://doi.org/10.1088/1742-6596/1402/4/044041

[21] Cho, E.E., Hein, H.H., Lynn, Z., Tran, T., Hla, S.J. (2019). Investigation on influence of infill pattern and layer thickness on mechanical strength of PLA material in 3D printing technology. Journal of Engineering and Science Research, 3(2): 27-37. https://doi.org/10.26666/rmp.jesr.2019.2.5

[22] Derise, M., Zulkharnain, A. (2020). Effect of infill pattern and density on tensile properties of 3D printed polylactic acid parts via fused deposition modeling (FDM). International Journal of Mechanical and Mechatronics Engineering IJMME-IJENS, 20(2): 54-62.

[23] Ma, Q., Rejab, M., Kumar, A., Fu, H., Kumer, N., Tang, J. (2020). Effect of infill pattern, density and material type of 3D printed cubic structure under quasi-static loading. Journal of Mechanical Engineering Science, 235(19): 1-19. https://doi.org/10.1177/0954406220971667

[24] Mahdi, H.H., Nama, S.A. (2022). Numerical investigation of free vibration for 3D printed functionally graded material cantilever beam. International Journal on Technical and Physical Problems of Engineering, 14(2): 27-35.

[25] Polylactic Acid (PLA, Polylactide). (2022). retrieved from https://www.makeitfrom.com/material-properties/Polylactic-Acid-PLA-Polylactide.